CMS Physics Analysis Summary

Contact: cms-pag-conveners-exotica@cern.ch 2014/03/12

Search for pair production of third-generation scalar leptoquarks and stops

The CMS Collaboration

Abstract

A search for pair production of heavy scalar particles is presented using events from a data sample of pp collisions corresponding to an integrated luminosity of 19.7 fb^{-1}, collected by the CMS detector at the LHC with $\sqrt{s} = 8$ TeV. The number of observed events is found to be in agreement with the standard model prediction. A 95% CL limit is set on the scalar particle pair production cross section times decay branching fraction. Third generation scalar leptoquarks with masses below 740 GeV are excluded at the 95% CL, assuming 100% braching fraction for the leptoquark decay to pair of a τ lepton and a b quark. This limit also directly constrains supersymmetric top partners, stops, decaying via an R-parity violating coupling λ'_{333}. A limit is also set on the cross section times branching fraction for stop pair production decaying via a mixture of both R-parity conserving and violating couplings. Stop quarks in this model with masses below 576 GeV are excluded at the 95% CL.

1 Introduction

Many extensions of the standard model (SM) predict new scalar or vector bosons, called leptoquarks (LQ), which carry non-zero lepton and baryon numbers, as well as color and fractional electric charge. Examples of such SM extensions include SU(5) grand unification [1], Pati-Salam SU(4) [2], composite models [3], superstrings [4], and technicolor [5] models. Leptoquarks decay to a quark and a charged lepton with a branching fraction that is model-dependent. Experimental limits on flavor-changing neutral currents and other rare processes favor leptoquarks that couple to quarks and leptons within the same SM generation, for leptoquark masses accessible to current colliders [3, 6].

The dominant pair-production mechanisms for leptoquarks at the Large Hadron Collider (LHC) are gluon-gluon fusion and quark-antiquark annihilation, and the cross sections for these processes depend only on the leptoquark mass and spin. In this report, a search for third-generation scalar leptoquarks, each decaying to a tau lepton and a b quark, is presented.

Similar signatures arising from supersymmetric models are also covered by this search. Supersymmetry (SUSY) is an attractive extension of the SM because it can resolve the hierarchy problem without unnatural fine-tuning, if the mass of the supersymmetric partner of the top quark (top squark, or stop) and the mass of the higgsinos are not too large [7]. In many natural SUSY models, the stop and higgsino are substantially lighter than the other scalar SUSY particles. In addition, a large mixing angle typically arises between the left-handed and right-handed chiral states of the stop, due to the large Yukawa coupling between the top and the Higgs boson. This produces two mass eigenstates, $\widetilde{t}_1$ and $\widetilde{t}_2$, with a large mass splitting. Thus, $M_{\widetilde{t}_1}$ can be significantly smaller than $M_{\widetilde{t}_2}$.

This light stop scenario can be realized in both R-parity conserving (RPC) and R-parity violating (RPV) SUSY models, where R-parity is a new, multiplicatively conserved quantum number [8] that distinguishes SM and SUSY particles. In the context of an RPC decay of the stop, the presence of an undetected particle (the lightest supersymmetric particle) is expected to generate a signature with large missing transverse momentum. If R-parity is violated, however, supersymmetric particles can decay into final states containing only standard model particles. The RPV terms in the superpotential are:

$$W \ni \frac{1}{2}\lambda_{ijk}L_iL_jE^c_k + \lambda'_{ijk}L_iQ_jD^c_k + \frac{1}{2}\lambda''_{ijk}U^c_iD^c_jD^c_k + \mu_iL_iH_u \qquad (1)$$

At the LHC, a $\widetilde{t}_1\bar{\widetilde{t}}_1$ pair is produced via strong interactions. When the masses of the supersymmetric partners of the gluon and quarks, excluding the top quark, are large, the stop pair production cross section is the same as that of the third generation LQ. The cross section also depends on the first-generation squark mass and the stop mixing angle because of loop corrections, but the contribution from these diagrams is less than 2%. In this search, two different decays of top squarks are considered. Both cases are simplified models with all of the other supersymmetric particles decoupled.

- The two-body lepton number violating decay $\widetilde{t}_1 \rightarrow \tau b$ [8] with a coupling constant λ'_{333} is allowed by the trilinear RPV operators. In this case, the final state signature and kinematics are identical to those from the pair production of third generation scalar leptoquarks. Thus, the results of an LQ3 search can be directly interpreted in the context of RPV stops. We search for stops with masses in the range 200 GeV to 1000 GeV.

- In some scenarios [9], the stop decay may preferentially proceed via superpartners, such as $\widetilde{t}_1 \to \tilde{\chi}^0 t$, $\widetilde{t}_1 \to \tilde{\chi}^{\pm} b$, etc., with the superpartner's decay involving one of the RPV operators. Such scenarios can occur if the higgsino, which is required to be light by naturalness, is lighter than the stop, or if the RPV couplings that allow direct decays are sufficiently small. We focus on a scenario in which the mass splitting between stop and chargino is $\sim$100 GeV. In this case, the dominant RPC decay of the stop is $\widetilde{t}_1 \to \tilde{\chi}^{\pm} b$. The chargino is assumed to be a pure higgsino and we consider the case when $\tilde{\chi}^{\pm} \to \tilde{\nu} + \tau^{\pm} \to jj + \tau^{\pm}$, $(m(\tilde{\nu}) = 2000\,\text{GeV})$. The latter decay occurs according to an RPV operator with a coupling constant λ'_{3jk}. Only the cases in which $j, k = 1, 2$ are considered. From such a signal process, we expect signatures with two τ leptons, two jets originating from hadronization of the b quarks, and at least four additional jets. Similarly to the LQ search, here as well two channels based on the different leptonic decays of one of the τ leptons are considered. We search for stops with masses in the range 300 GeV to 900 GeV.

  Another decay of chargino to $\nu + \tilde{\tau}$ through the λ'_{3jk} coupling is highly suppressed due to chirality as the chargino must decay to $\nu_L + \tilde{\tau}_R$, while $\tilde{\tau}_R$ is not part of the L superfield. Therefore, decays through this coupling do not produce events with large missing transverse energy and are not covered by other searches.

The data sample used in this search has been recorded by the CMS detector and corresponds to an integrated luminosity of 19.7 fb^{-1} of pp collisions at a center-of-mass energy of 8 TeV. One of the τ leptons in the final state is required to decay leptonically: $\tau \to \ell \nu_\ell \nu_\tau$, where ℓ can be either a muon or an electron, denoted as a light lepton. The other τ lepton is required to decay to hadrons (τ_h): $\tau \to \text{hadrons} + \nu_\tau$. Additionally, at least two more jets expected to originate from hadronization of the two b quarks are required. These requirements result in two possible final states labeled below as $e\tau_h$ and $\mu\tau_h$, or $\ell\tau_h$. In this report, the search for scalar leptoquarks and stops decaying through the coupling λ'_{333}, which have the same final state and kinematics, is called the leptoquark search. The search for the chargino-mediated decay of stops involving the λ'_{3jk} coupling is called the stop search.

No evidence for third generation leptoquarks or stops has been found in previous searches, using a final state with a τ_h, a light lepton, and b jets. The most stringent lower limit to date on the mass of scalar third generation leptoquarks decaying to pair of a τ lepton and a b quark with 100% branching fraction is at $\sim$530 GeV from both the ATLAS [10] and CMS [11] experiments. This is the first search for the chargino-mediated decay of the stop through the RPV coupling λ'_{3jk}.

2 CMS detector

The central feature of the CMS apparatus is a superconducting solenoid, of 6 m internal diameter, providing a field of 3.8 T. Within the field volume are several subdetectors. A silicon pixel and strip tracker allows the reconstruction of the trajectories of charged particles within the pseudorapidity range $|\eta| < 2.5$, where $\eta = -\ln\tan(\theta/2)$ and θ is the polar angle. The calorimetry system consists of a lead tungstate crystal electromagnetic calorimeter (ECAL) and a brass/scintillator hadron calorimeter (HCAL), and measures particle energy depositions for $|\eta| < 3$. CMS also has extensive forward calorimetry. Muons are measured in gas-ionization detectors embedded in the steel return yoke. Collision events are selected using a two-tiered trigger system [12]. A more detailed description of the CMS detector can be found in [13].

3 Trigger and event selection

Candidate LQ or stop events were collected using a set of triggers requiring the presence of either an electron or a muon with transverse momentum thresholds of 27 GeV and 24 GeV, respectively.

Electrons are reconstructed within the geometrical acceptance $|\eta| < 2.1$ using information from the ECAL and the tracker. Selected electrons are required to have transverse momenta $p_T > 30\,\text{GeV}$, an electromagnetic shower shape consistent with that of an electron, and an energy deposition in ECAL that is compatible with the track reconstructed in the tracker. Muons are required to be reconstructed by both the tracker and the muon spectrometer. They are required to have $|\eta| < 2.1$ and $p_T > 30\,\text{GeV}$. A particle-flow (PF) technique [14–16] is used for the reconstruction of hadronically decaying τ_h candidates. In the PF approach, information from all subdetectors is combined to reconstruct and identify all final-state particles produced in the collision. The particles are classified as either charged hadrons, neutral hadrons, electrons, muons, or photons. These particles are used with the hadron plus strip (HPS) algorithm [17] to identify τ_h objects. Hadronic decays of taus with one or three charged pions and up to two neutral pions are reconstructed. The reconstructed τ_h is required to have $p_T > 50\,\text{GeV}$ and $|\eta| < 2.3$. Selected electrons, muons, and taus are required to be isolated from other reconstructed particles. The identified electron (muon) and τ_h are required to originate from the same vertex and be separated spatially by $\Delta R \equiv \sqrt{\Delta\phi^2 + \Delta\eta^2} > 0.5$. The lepton and the τ_h are also required to have opposite electric charge. Events containing additional light leptons with an opposite electric charge from the already selected light lepton are vetoed.

Jets are reconstructed with the anti-k_t algorithm with a size parameter $R = 0.5$ [18, 19] using PF candidates. Jet energies are corrected by subtracting the average contribution from particles from other proton-proton collisions in the same beam crossing (pileup) and by correcting the jet momentum to better reflect the true total momentum of the particles in the jet [20]. Selected jets are required to be within $|\eta| < 2.4$ and have $p_T > 30$ GeV, and to be separated from the selected electron or muon and the τ_h by $\Delta R > 0.5$.

The search for leptoquarks is performed in a sample of events containing one light lepton (electron or muon for $e\tau_h$ and $\mu\tau_h$ channels, respectively), a hadronically decaying tau, and at least two jets, with at least one of the jets identified as originating from b-quark hadronization (b-tagged) using the combined secondary vertex (CSV) algorithm [21]. To discriminate between signal and background, the mass of the τ_h and a jet ($M(\tau_h, j)$) is required to be greater than 250 GeV. There are two possible pairings of the tau with a jet. The pairing is chosen to minimize the difference between the mass of the tau and one jet and the mass of the lepton and the other jet:

$$\{m, n\} : \min[|M(\tau_h, j_m) - M(\ell, j_n)|], \{m, n\} = \{1, 2\}, m \neq n \tag{2}$$

The search for stop quark pair production is performed in a sample of events containing one light lepton (electron or muon for $e\tau_h$ and $\mu\tau_h$ channels, respectively), a hadronically decaying tau, and at least five jets, with at least one of the jets b-tagged using the CSV algorithm.

The S_T distribution after the final selection is used to extract the limits on both the leptoquark and stop signal scenarios, where S_T is defined as the scalar sum of transverse momentum for all required final state objects in each search.

$$S_{\mathrm{T}}^{(\mathrm{LQ})} = p_{\mathrm{T}}(\ell) + p_{\mathrm{T}}(\tau_{\mathrm{h}}) + p_{\mathrm{T}}(\text{b-jet}) + p_{\mathrm{T}}(\text{jet}) \quad (3)$$

$$S_{\mathrm{T}}^{(\mathrm{stop})} = p_{\mathrm{T}}(\ell) + p_{\mathrm{T}}(\tau_{\mathrm{h}}) + p_{\mathrm{T}}(\text{b-jet}) + \sum_{i=1}^{4} p_{\mathrm{T}}(\text{jet } i) \quad (4)$$

4 Background and Signal Models

Several standard model processes can mimic the final state signatures expected from leptoquark or stop pair production and decay. The major irreducible background process is the pair production of top quarks ($\mathrm{t\bar{t}}$) when both the light lepton and τ_{h} are produced from decays of genuine τ leptons. The major reducible background consists of events in which a jet is misidentified as a hadronically decaying tau. The processes that contribute to this background are mainly associated production of a W or Z boson with jets, and $\mathrm{t\bar{t}}$. Additionally, there is a small contribution to this background from the QCD multijet process. Small contributions from diboson and single top processes, and from $\mathrm{t\bar{t}}$ and Z+jets processes when a light lepton is misidentified as a τ_{h}, are estimated from simulation.

The PYTHIA v6.4 generator [22] is used to model the signal and diboson processes. The leptoquark signal samples are generated with masses ranging from 400 GeV to 1000 GeV, and the stop signal samples are generated with masses ranging from 300 GeV to 800 GeV. The MADGRAPH generator [23] is used to model the $\mathrm{t\bar{t}}$, W+jets, and Z+jets processes. The single top production is modeled with the POWHEG [24] generator. Both MADGRAPH and POWHEG generators are interfaced with PYTHIA v4.6 for hadronization and showering. The TAUOLA program [25] is used for tau lepton decay in the leptoquark, $\mathrm{t\bar{t}}$, W+jets, Z+jets, diboson, and single top processes. Each sample is passed through a full simulation of the CMS detector based on GEANT4 [26] and the complete set of reconstruction algorithms used to analyze collision data. Theoretical cross sections are used to normalize the simulated samples. Cross sections for the signal and diboson processes are calculated to next-to-leading order [27]. The next-to-next-to-leading order [28–30] cross sections are used to normalize the rest of the background processes. The contribution from the QCD multijet process is estimated from data control samples.

The efficiencies of the trigger and final selection criteria for signal processes are estimated from the simulation. The identification efficiencies for leptons and b jets are calculated from data collected in different periods, and used where necessary to correct the event selection efficiency estimations from the simulation.

The $\mathrm{t\bar{t}}$ irreducible background is estimated from the observed $e\mu$ sample. Selected events are required to contain one electron, one muon, and satisfy the remaining final selection criteria, except that a τ_{h} is not required. The signal contamination of this sample has been found to be negligible for any signal mass hypothesis. The final yield of the $e\mu$ sample is scaled by the relative difference of the selection efficiencies between the $\ell\tau_{\mathrm{h}}$ and $e\mu$ samples. The selection efficiencies are measured in the simulation and are corrected to match those from data. The data-driven estimation of the final yield agrees with both the direct prediction from the simulation and the yield obtained after applying the same method to the MC samples. Systematic uncertainties are assigned to the final yield based on statistical uncertainty in the control samples and on the propagation of the uncertainties on the acceptances, efficiencies, and scale factors. The S_{T} distribution for this background is obtained from the simulated $\mathrm{t\bar{t}}$ sample consisting exclusively of fully leptonic decays of top quarks.

The reducible background from $\mathrm{t\bar{t}}$, W+jets, and Z+jets events in which a jet is misidentified as a hadronically decaying tau is estimated from observed data. The probability of misidentification is measured using events recorded with a Z boson produced in association with jets and decaying to a pair of muons ($Z \to \mu\mu$). The invariant mass of the muon pair is required to be greater than 50 GeV and events are required to contain at least one τ_h candidate, which may or may not pass the usual isolation requirement. The misidentification probability is calculated as the fraction of τ_h candidates which pass the isolation requirement and depends on the transverse momentum of the candidates. The background yield is estimated from a sample of events satisfying the final selection criteria, except that all τ_h candidates in the events must fail the isolation requirement. The anti-isolated events are weighted by a function of the misidentification probability, as given in Eq. (5):

$$N^{(\text{main})}_{\text{misID } \tau} = \sum_{\text{events}}^{(\text{anti-iso})} \frac{1 - \prod_\tau [1 - f(p_T(\tau))]}{\prod_\tau [1 - f(p_T(\tau))]} \tag{5}$$

where the misidentification probability is denoted as $f(p_T)$. The data-driven estimation of the yield agrees with both the direct prediction from the simulation and the estimation performed using the same approach on simulated samples. The major sources of systematic uncertainty on the final background yield are the statistical uncertainty on the misidentification probability, the estimated difference in the misidentification probability for $t\bar{t}$ events, and the variation of the misidentification probability when requiring the presence of additional jets, separate from the τ_h candidates used in the probability calculation, in the $Z \to \mu\mu$ control sample. The S_T distribution for this background is obtained using simulated samples, consisting of events where a jet is misidentified as a τ_h, for the W+jets and Z+jets processes and the $t\bar{t}$ process with exclusively semi-leptonic decays.

The QCD multijet process contributes only in the $e\tau_h$ channel. The contribution from QCD events is estimated from a data sample satisfying the final selection criteria for the $e\tau_h$ channel except that the electron and τ_h must have the same electric charge. The QCD component is included in the distribution of the rest of the reducible background, described above.

5 Systematic uncertainties

The estimations of the background and the signal efficiency are affected by systematic uncertainties. The uncertainty on the total integrated luminosity is 2.6% [31]. The uncertainty on the trigger and lepton efficiencies is 2%, while the uncertainty assigned to the τ_h identification efficiency is 6%. The uncertainties on the b-tagging efficiency and mistagging probability depend on pseudorapidity and transverse momentum and are on average 4% and 10%, respectively. Systematic uncertainties on the normalization of the major backgrounds are 19-22% for the irreducible background and 16-24% for the reducible background. Due to the limited number of events in the simulation, uncertainties on small backgrounds range between 20-50%. A 4% uncertainty, due to modeling of initial- and final-state radiation in the simulation, is assigned to the signal acceptance. Uncertainty due to the effect of pileup modeling in the MC is estimated to be 3%. Jet energy scale uncertainties (2-4% depending on pseudorapidity and transverse momentum) and energy resolution uncertainties (5-10% depending on transverse momentum), as well as energy scale (3%) and resolution (10%) uncertainties for τ_h, affect both the S_T distribution and the expected yields from the signal and background processes. All of these effects are taken into account.

6 Results

The number of observed events and expected signal and background events after the final selection for the leptoquark and stop searches are listed in Table 1 and Table 2, respectively. The S_T distribution of the selected events in data and simulation, combining $e\tau_h$ and $\mu\tau_h$ channels, are shown in Fig. 1 for the LQ search and Fig. 2 for the stop search. The LQ signal tends to have more events in the tail of S_T distribution than the backgrounds. The stop signal shows a visible enhancement above the backgrounds in the core of the S_T distribution. As the data agree well with the SM background prediction, a limit is set on the product of the cross section for pair production of third-generation LQs (stops) and the square of the branching fraction, B, for the LQ decay to a τ lepton and a b quark (stop decay to a $\chi^{\pm}$ and a b quark, with a subsequent decay of the chargino via $\tilde{\chi}^{\pm} \rightarrow \tilde{\nu} + \tau^{\pm} \rightarrow jj + \tau^{\pm}$). The modified frequentist construction CL_s [32, 33] is used for the limit calculation. A maximum likelihood fit is performed to the S_T spectrum simultaneously for both the $e\tau_h$ and $\mu\tau_h$ channels, taking into account correlations between the systematic uncertainties. Expected and observed limits as a function of the signal mass are shown in Fig. 3 for the LQ search and Fig. 5 for the stop search. Similar results are obtained when calculating limits using a Bayesian method with a flat prior. These limits assume $B = 100\%$. The limits for the LQ search as a function of the leptoquark branching ratio and the mass are shown in Fig. 4. We exclude scalar leptoquarks with masses below 740 GeV, in good agreement with the expected exclusion at 754 GeV. We exclude stop quarks with masses below 576 GeV, in agreement with the expected exclusion at 588 GeV.

Table 1: Observed event yields, estimated backgrounds, and expected number of signal events for the LQ search. Uncertainties on simulation-based estimations are given as $\pm$ (statistical uncertainty) $\pm$ (systematic uncertainty), where the latter includes the systematic uncertainties affecting yields.

	$\mu\tau_h$ Channel	$e\tau_h$ Channel
$t\bar{t}$ (irreducible)	66.7 ± 12.6	105.6 ± 18.1
Reducible	117.3 ± 18.9	147.8 ± 33.0
$Z(\ell\ell/\tau\tau)$+jets	$7.5 \pm 4.6 \pm 0.2$	$21.4 \pm 7.4 \pm 4.9$
Single-t	$17.3 \pm 2.8 \pm 4.7$	$16.0 \pm 2.8 \pm 4.4$
VV	$2.6 \pm 0.5 \pm 0.8$	$4.1 \pm 0.6 \pm 1.3$
Total Bkg.	$211.4 \pm 5.4 \pm 23.4$	$294.9 \pm 7.9 \pm 39.1$
Observed	216	289
Signal (500 GeV)	$51.6 \pm 1.3 \pm 5.3$	$57.7 \pm 1.4 \pm 5.9$
Signal (600 GeV)	$17.7 \pm 0.4 \pm 1.6$	$20.1 \pm 0.5 \pm 1.9$
Signal (700 GeV)	$6.2 \pm 0.1 \pm 5.5$	$7.1 \pm 0.2 \pm 6.3$
Signal (800 GeV)	$2.3 \pm 0.1 \pm 0.2$	$2.7 \pm 0.1 \pm 0.2$

In summary, a search for pair production of third-generation scalar leptoquarks and top squarks has been presented. The leptoquark search is performed in the final state including an electron or a muon, a hadronically decaying τ lepton, and at least two jets, one of which is b-tagged. The stop search is performed in events containing an electron or a muon, a hadronically decaying τ lepton, and at least five jets, one of which is b-tagged. No excesses above the SM background prediction are observed in the S_T distributions. Assuming a 100% branching fraction for the decays of the hypothetical particles, the existence of the scalar leptoquarks with masses below 740 GeV and top squarks with masses below 576 GeV is excluded at the 95% CL. The limits on the leptoquarks are the most stringent to date, while this is the first search for top squarks in such a final state.

Table 2: Observed event yields, estimated backgrounds, and expected number of signal events for the stop search. Uncertainties on simulation-based estimations are given as ± (statistical uncertainty) ± (systematic uncertainty), where the latter includes the systematic uncertainties affecting yields.

	$\mu\tau_h$ Channel	$e\tau_h$ Channel
$t\bar{t}$ (irreducible)	55.0 ± 9.5	88.3 ± 13.7
Reducible	59.8 ± 13.8	65.7 ± 16.4
$Z(\ell\ell/\tau\tau)$+jets	$11.6 \pm 5.5 \pm 2.7$	$4.9 \pm 2.5 \pm$
Single-t	$3.5 \pm 1.3 \pm 0.9$	$3.9 \pm 1.5 \pm$
VV	$0.4 \pm 0.2 \pm 0.1$	$0.6 \pm 0.2 \pm 0.2$
Total Bkg.	$130.3 \pm 5.6 \pm 17.1$	$162.5 \pm 2.9 \pm 21.5$
Observed	123	156
Signal (300 GeV)	$82.8 \pm 8.0 \pm 11.7$	$94.3 \pm 8.5 \pm 13.2$
Signal (400 GeV)	$38.3 \pm 2.3 \pm 3.8$	$43.9 \pm 2.6 \pm 4.3$
Signal (500 GeV)	$15.4 \pm 0.7 \pm 1.5$	$19.4 \pm 0.8 \pm 1.8$
Signal (600 GeV)	$5.7 \pm 0.3 \pm 0.5$	$6.9 \pm 0.9 \pm 0.7$

References

[1] H. Georgi and S. L. Glashow, "Unity of All Elementary-Particle Forces", *Phys. Rev. Lett.* **32** (Feb, 1974) 438–441, doi:10.1103/PhysRevLett.32.438.

[2] J. C. Pati and A. Salam, "Lepton number as the fourth "color"", *Phys. Rev. D* **10** (Jul, 1974) 275–289, doi:10.1103/PhysRevD.10.275.

[3] B. Gripaios, "Composite leptoquarks at the LHC", *Journal of High Energy Physics* **2010** (2010) 1–18. 10.1007/JHEP02(2010)045.

[4] J. L. Hewett and T. G. Rizzo, "Low-Energy Phenomenology of Superstring Inspired E(6) Models", *Phys.Rept.* **183** (1989) 193, doi:10.1016/0370-1573(89)90071-9.

[5] E. Eichten and K. Lane, "Dynamical breaking of weak interaction symmetries", *Physics Letters B* **90** (1980), no. 12, 125 – 130, doi:10.1016/0370-2693(80)90065-9.

[6] O. Shanker, "$\pi\ell2$, $K\ell3$, and $K^0 - \overline{K}^0$ constraints on leptoquarks and supersymmetric particles", *Nuclear Physics B* **204** (1982), no. 3, 375 – 386, doi:10.1016/0550-3213(82)90196-1.

[7] M. Papucci, J. T. Ruderman, and A. Weiler, "Natural SUSY Endures", *JHEP* **09** (2012) 035, doi:10.1007/JHEP09(2012)035, arXiv:1110.6926.

[8] R. Barbier et al., "R-Parity-violating supersymmetry", *Physics Reports* **420** (2005), no. 16, 1 – 195, doi:10.1016/j.physrep.2005.08.006.

[9] J. Evans and Y. Kats, "LHC searches examined via the RPV MSSM", in *The 2013 European Physical Society Conference on High Energy Physics*. SISSA, 2013. arXiv:1311.0890. PoS(EPS2013)287.

[10] ATLAS Collaboration, "Search for third generation scalar leptoquarks in pp collisions at $\sqrt{s} = 7$TeV with ATLAS detector", *JHEP* **06** (2013) 033, doi:10.1007/JHEP06(2013)033, arXiv:1303.0526.

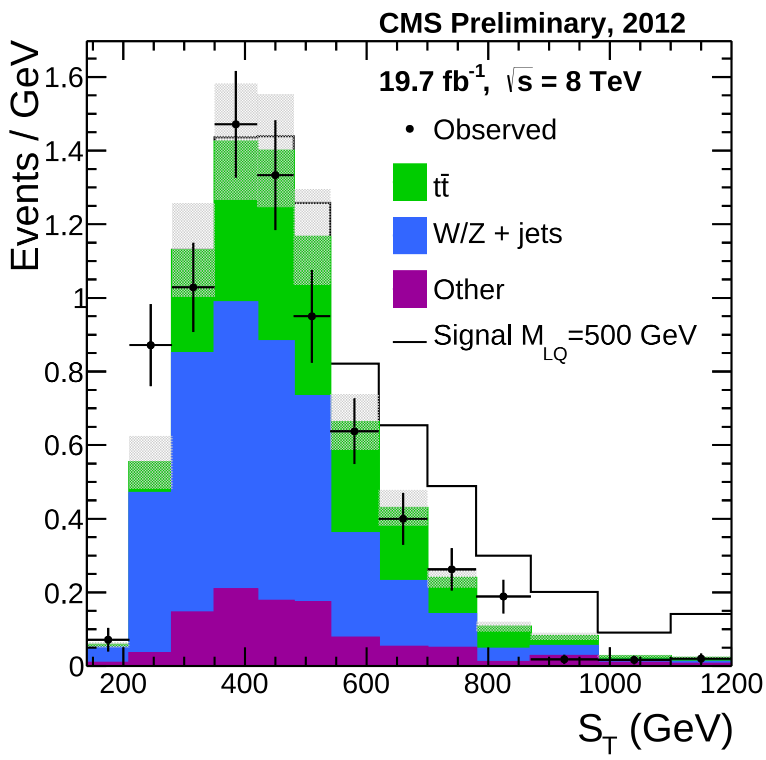

Figure 1: Final S_T distribution for the LQ search with the $e\tau_h$ and $\mu\tau_h$ channels combined. A signal sample for leptoquarks at a mass of 500 GeV is added on top of the background prediction. The last bin contains the overflow events. Gray uncertainty band corresponds to the systematic uncertainties due to background estimation.

[11] CMS Collaboration, "Search for third generation leptoquarks and top squarks decaying to a τ lepton and a b quark in pp collisions at $\sqrt{s} = 7$ TeV", *Phys. Rev. Lett.* **110** (2013) 081801, doi:10.1103/PhysRevLett.110.081801, arXiv:1210.5629.

[12] CMS Collaboration, "The CMS high level trigger", *Eur. Phys. J. C* **46** (2006) 605, doi:10.1140/epjc/s2006-02495-8.

[13] CMS Collaboration, "The CMS experiment at the CERN LHC", *JINST* **3** (2008) S08004, doi:10.1088/1748-0221/3/08/S08004.

[14] CMS Collaboration, "Particle Flow Event Reconstruction in CMS and Performance for Jets, Taus, and MET". CMS PAS-PFT-09-001.

[15] CMS Collaboration, "Commissioning of the Particle-Flow Reconstruction in Minimum-Bias and Jet Events from pp Collisions at 7 TeV", CMS Physics Analysis Summary CMS-PAS-PFT-10-002, 2010.

[16] CMS Collaboration, "Commissioning of the particle-flow event reconstruction with leptons from J/Ψ and W decays at 7 TeV", CMS Physics Analysis Summary CMS-PAS-PFT-10-003, 2010.

[17] CMS Collaboration, "Performance of tau-lepton reconstruction and identification in CMS", *JINST* **7** (2012) 01001, doi:10.1088/1748-0221/7/01/P01001.

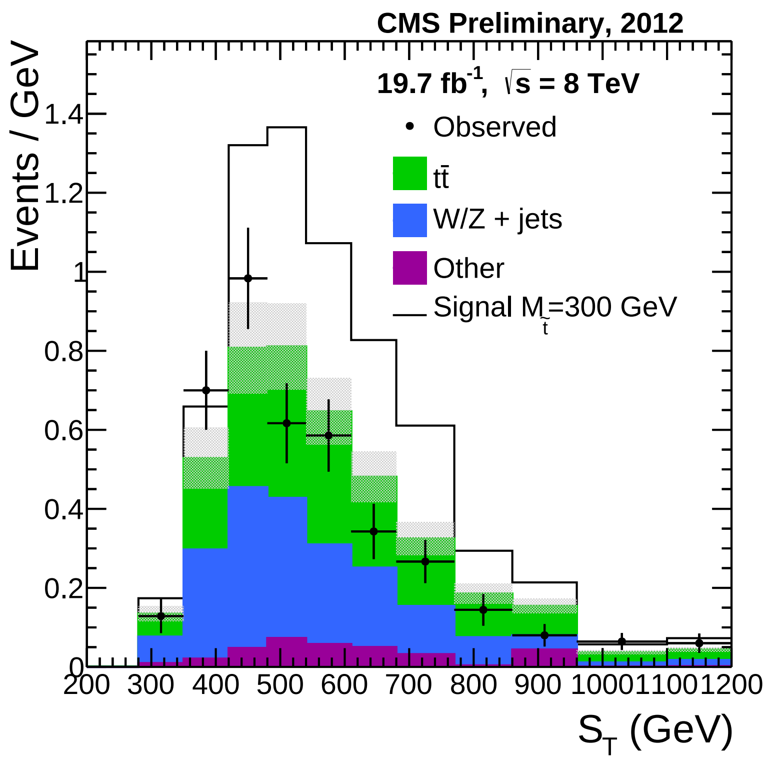

Figure 2: Final S_T distribution for the stop search with the $e\tau_h$ and $\mu\tau_h$ channels combined. A signal sample for stops at a mass of 300 GeV is added on top of the background prediction. The last bin contains the overflow events. Gray uncertainty band corresponds to the systematic uncertainties due to background estimation.

[18] G. P. Salam, "Towards Jetography", *Eur. Phys. J.* **C67** (2010) 637–686, doi:10.1140/epjc/s10052-010-1314-6.

[19] M. Cacciari, G. P. Salam, and G. Soyez, "The anti-k_t jet clustering algorithm", *JHEP* **04** (2008) 063, doi:10.1088/1126-6708/2008/04/063, arXiv:0802.1189.

[20] CMS Collaboration, "Determination of Jet Energy Calibration and Transverse Momentum Resolution in CMS", *JINST* **6** (2011) 11002, doi:10.1088/1748-0221/6/11/P11002.

[21] CMS Collaboration, "Identification of b-quark jets with the CMS experiment", *JINST* **8** (2013) P04013, doi:10.1088/1748-0221/8/04/P04013, arXiv:1211.4462.

[22] T. Sjöstrand, S. Mrenna, and P. Skands, "PYTHIA 6.4 physics and manual", *JHEP* **05** (2006) 026, doi:10.1088/1126-6708/2006/05/026, arXiv:hep-ph/0603175.

[23] J. Alwall *et al.*, "MadGraph/MadEvent v4: The New Web Generation", *JHEP* **09** (2007) 028, doi:10.1088/1126-6708/2007/09/028, arXiv:0706.2334.

[24] S. Frixione, P. Nason, C. Oleari, "Matching NLO QCD computations with parton shower simulations: the POWHEG method", *JHEP* **11** (2007) 070, doi:10.1088/1126-6708/2007/11/070, arXiv:0709.2092.

[25] Z. Wąs, "TAUOLA the library for tau lepton decay, and KKMC/KORALB/KORALZ...status report", *Nucl. Phys. B, Proc. Suppl.* **98** (2001) 96, doi:10.1016/S0920-5632(01)01200-2.

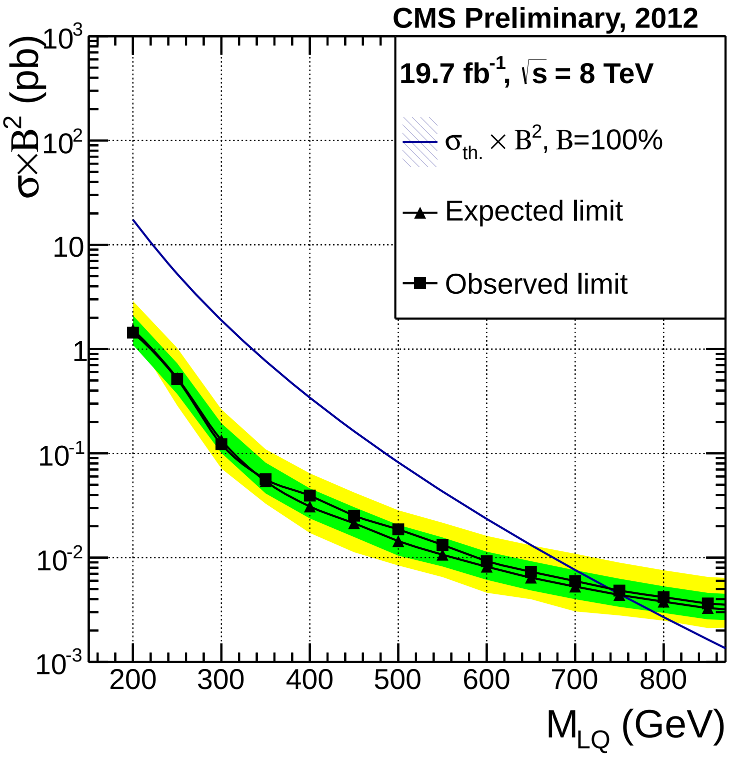

Figure 3: The expected and observed combined upper limit on the LQ pair production cross section times B^2 at the 95% CL, as a function of the LQ mass. The dark blue curve and the light blue band represent the theoretical LQ pair production cross section and the uncertainties due to the choice of PDF and renormalization/factorization scales.

[26] S. Agostinelli et al., "Geant4—a simulation toolkit", *Nucl. Instrum. Meth. A* **506** (2003) 250, doi:10.1016/S0168-9002(03)01368-8.

[27] M. Krämer, T. Plehn, M. Spira, and P. M. Zerwas, "Pair production of scalar leptoquarks at the CERN LHC", *Phys. Rev. D* **71** (2005) 057503, doi:10.1103/PhysRevD.71.057503, arXiv:hep-ph/0411038.

[28] K. Melnikov and F. Petriello, "Electroweak gauge boson production at hadron colliders through O(α_s^2)", *Phys. Rev. D* **74** (2006) 114017, doi:10.1103/PhysRevD.74.114017, arXiv:hep-ph/0609070.

[29] R. Kleiss and W. J. Stirling, "Top quark production at hadron colliders: Some usefulformulae", *Z. Phys.* **C 40** (1988) 419–423, doi:10.1007/BF01548856.

[30] CMS Collaboration, "Measurement of W^+W^- production and search for the Higgs boson in pp collisions at $\sqrt{s} = 7$ TeV", *Phys. Lett. B* **699** (2011) 25, doi:10.1016/j.physletb.2011.03.056.

[31] CMS Collaboration, "Measurement of CMS Luminosity", CMS Physics Analysis Summary CMS-PAS-EWK-10-004, 2010.

[32] A. L. Read, "Modified frequentist analysis of search results (the CLs method)", CERN Report CERN-OPEN-2000-005, 2000.

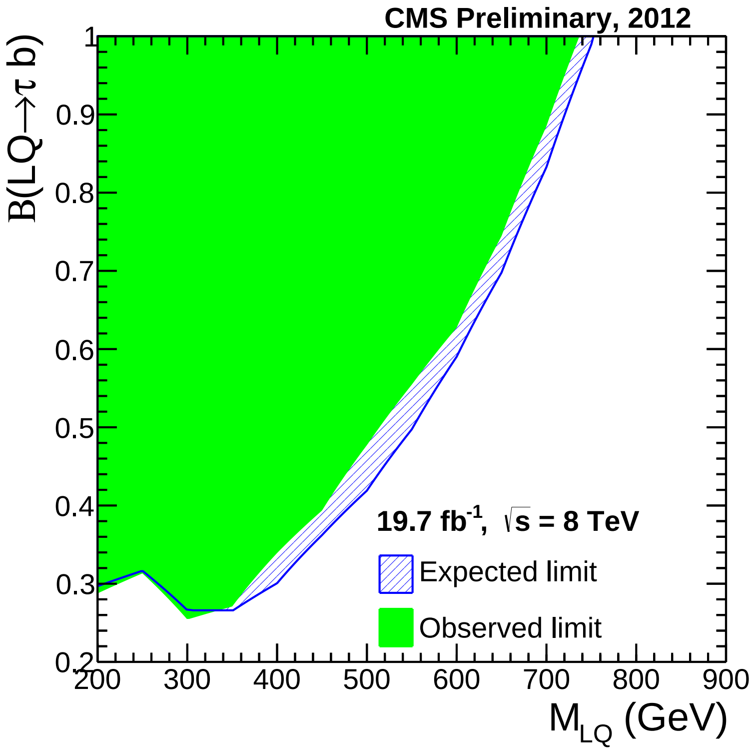

Figure 4: Expected (dashed blue) and observed (green solid) 95% C.L. limit on the branching ratio for the leptoquark decay to a tau lepton and a b quark, as a function of the leptoquark mass.

[33] ATLAS and CMS Collaborations, LHC Higgs Combination Group, "Procedure for the LHC Higgs boson search combination in Summer 2011", ATL-PHYS-PUB/CMS NOTE 2011-11, 2011/005, 2011.

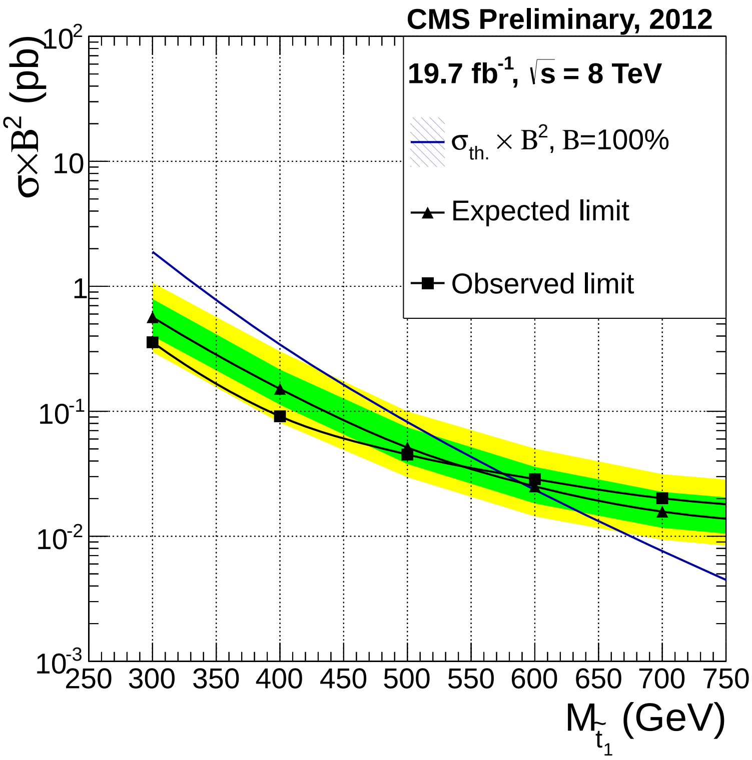

Figure 5: The expected and observed combined upper limit on the stop pair production cross section times B^2 at the 95% CL, as a function of the stop mass. The dark blue curve and the light blue band represent the theoretical stop pair production cross section and the uncertainties due to the choice of PDF and renormalization/factorization scales.